Cost-Effective Optimal Synthesis of the Efficiency Map of Permanent Magnet Synchronous Motors

Paolo Di Barba[1], Maria Evelina Mognaschi[1], Lidija Petkovska[2], Goga Cvetkovski[2]

[1] Dept of Electrical, Computer and Biomedical Engineering
University of Pavia
Pavia, Italy
{paolo.dibarba, eve.mognaschi}@unipv.it

[2] Faculty of Electrical Engineering and IT
Ss Cyril&Methodius University
Skopje, North Macedonia
{lidijap, gogacvet}@feit.ukim.edu.mk

***Abstract*—In the paper an original approach to efficiency map optimal synthesis is presented. A permanent magnet motor, working as standard AC motor of synchronous type (PMSM) is selected as the case study. The first target of this research is to derive a lumped-parameter model of the motor (low-fidelity model), validated by magnetic field analysis (high-fidelity model). In turn, the end target is its application in a cost-effective optimisation procedures, where the goal is to identify the motor geometry maximizing the map area which is encompassed by a prescribed value for the motor efficiency.**

Keywords—permanent magnet synchronous motor (PMSM), efficiency map, shape optimisation, lumped-parameter model, magnetic field analysis

Introduction

Permanent magnet (PM) motors working either as brushless DC motors (PMBLDC) or as synchronous AC motors (PMSM) are becoming much sought-after due to their superior performance characteristics, smooth control and higher energy efficiency. Recently, the topology of permanent magnet motors is under reconsideration and new, attractive topologies for improved performance motors and with improved efficiency values are developing.

The motor performance depends on many different factors which determine the electromagnetic properties and field distribution inside the motor domain. When designing a particular motor, then the supplying conditions and the load conditions are input parameters, which are defined and known in advance. The main task of an electric motor designer is, for given objective function, to find the optimal design, getting the best possible motor performance at the least material usage, and satisfying given criteria and prescribed physical or technical limitations.

For solving electric motor optimisation problems, so far, a great deal of research work has been done [1]. However one notable issue has not been observed yet, and a lack of elaboration in the literature is evident. The authors of this paper find that optimisation of a motor performance, through optimisation of the efficiency map area and shape, is a challenging and promising piece of research work.

It is anticipated that the optimisation of a torque-speed (*T-n)* efficiency map for an electric motor, where the considered design variables are dimensions of the motor geometry, will lead to a more effective motor operation. In this sense, a meaningful issue to study is not only to improve the shape of the efficiency map, but also, even more important criterion, idea is to broaden the covered *T-n* area for given bound on the motor efficiency η.

The key step in this task is certainly reliable and accurate synthesis of the efficiency map for a studied electric motor. After a map synthesis is completed a thorough analysis of its main features is accomplished, the optimisation problem is defined and the objective function is selected. The key idea is to shape the efficiency map contour lines in the torque-speed plane by controlling the motor geometry through an algorithm of evolutionary computing. The second idea is to exploit a multi-fidelity model for the magnetic analysis of the motor in view of a cost-effective procedure. Accordingly, in the paper an original approach to the efficiency map synthesis is presented. The paper is organized as follows: the case study description followed by the performance analysis, is first presented and a further section is dedicated to the description of the efficiency map calculation. Subsequently, the optimization problem is stated and the results are shown. Finally, a conclusion is draw.

Case study – PMSM

Performance specifications and requirements for higher energy efficiency are vital for application of electrical machines. To improve motor performance and efficiency are of great significance to energy sustainability and environment protection. This goal is achieved by shape design and optimization of electric motors. The proposed procedure for efficiency map synthesis and optimisation is applied on a permanent magnet synchronous motor (PMSM) type EKM 90M-6 produced by Koncar company. The drive can work in two typical operating regimes:

(a) as a standard permanent magnet synchronous (PMSM) motor supplied by a three sinewave phase AC source, having the rated data U_n = 42 V@50 Hz, I_n = 17.6 A, n_n = 1000 rpm, T_n = 10 Nm, η = 0.848;

(b) as a brushless DC permanent magnet (BLDCPM) motor, typically working as low inertia servomotor with torque control 0-10 Nm and speed control 0-4000 rpm, supplied by a six-pulse transistor bridge inverter with rectangular current waves [2].

In order to encompass the whole (*T*,*n*) operating space of the PMSM, the efficiency map will be sinthesised and then optimised for the regime (b) which is here taken as *case study*. For the power supply is used a six-pulse current inverter, and hence the six poles topology is the best suited. Thus, the studied motor is with 36 slots of the stator core lamination, while on the rotor are placed 6 surface mounted samarium-cobalt permanent magnets, that are radially magnetized. The material is SmCo5, with remanence B_r = 0.95 T and coercivity H_c = –720 kA/m. In the stator slots there are placed three single-layer Y-connected phase windings. As the studied motor foremost serves as a low-inertia servomotor – in order to reduce the rotor mass – on the rotor are designed six holes symmetrically positioned to the permanent magnets. In Fig. 1 the cross-section of motor lamination with stator windings is depicted.

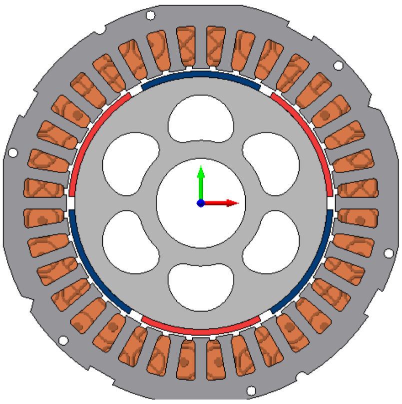

Fig. 1. Permanent magnet synchronous motor (PMSM) lamination

An important part of the proposed methodology for a synthesis and optimisation of the efficiency map for the investigated motor are FEA based analyses. To perform accurate FEM calculations, the detailed geometry design topology and properties of the used materials is a prerequisite. In Fig. 2 the magnetising characteristics for the electrical steel used for stator and rotor cores are presented.

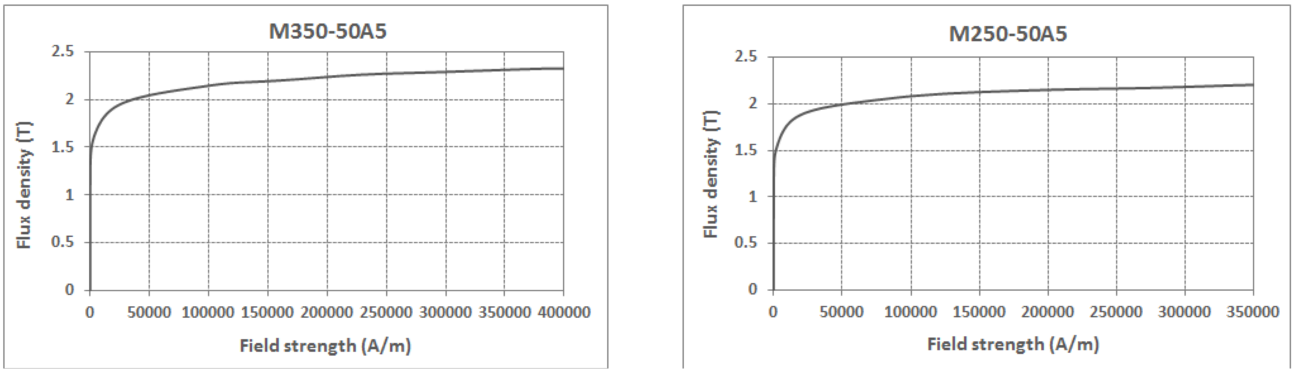

(a) (b)

Fig. 2. B-H curves for the stator core (a) and rotor core (b)

The analysis problem

The strategy for efficiency map synthesis is based on two models of the motor: a low-fidelity (LF) model and a high-fidelity (HF) one, respectively. The LF model (usually an analytical model) is used to calculate parameters and performance characteristics of the PMSM; in turn, the HF model is subsequently used to validate the results from the LF model is applied to validate the results of the first one.

Development of a circuit model for simple and fast analytical calculation of parameters and characteristics for an electric motor has always been a challenging issue for researchers [3,4]. However, due to specific features of each particular motor, there do not exist general models that are directly applicable to the case studies. Because of that, the first step to the analysis problem in this research work is to develop a respective mathematical model for the analysed PMSM.

The analytical LF model development of the permanent magnet motor is based on a system of mutually related equations, where only the preselected design variables are independent. Later they are used to carry out optimisation of the efficiency map in *T*×*n* design space, the target of this research work. The outcome is a new set of optimal design variables, providing higher efficiency in an extended map area. The motor performance parameters and characteristics, are dependent only on the variables from the selected set, all they being developed at a given shaft torque T and a rotor speed $n \equiv \omega$. This way, the LF analytical model for PMSM is directly applicable both for calculation of the points on the efficiency map space and for solving the optimisation problem. From the bulk of equations describing the motor model, only the more important equations are presented, in continuation.

The widely known expression for efficiency calculation is:

$$Efficiency = \eta = \frac{P_2}{P_1} = \frac{P_2}{P_2 + P_{loss}} \tag{1}$$

Where the output power P_2 is determined with:

$$P_2 = T \cdot \omega = f(T, \omega) \tag{2}$$

While the requested rotor speed ω is obtained by the respective source frequency f_s.

$$\omega = f(f_s) \quad \rightarrow \quad f_s = f(\omega) \tag{3}$$

First, let to underline that the air-gap flux density B_g at no-load in PM motors, is dependent only of the gap geometry and the flux created by the permanent magnets Φ_{PM}. Hence, for a given set of design variables it is:

$$B_g \equiv \Phi_{PM} = \text{cons.} \tag{4}$$

Knowing from theory that the requested shaft toque is dependent on the air-gap flux and winding current, in accordance with eq. (4) follows:

$$T = f(I) \quad \rightarrow \quad I = f(T) \tag{5}$$

The total loss in eq. (1) is consisted of three components: copper loss – P_{Cu}, iron loss – P_{Fe} and mechanical (friction and windage) loss – P_{fw}. Considering the eqs. (3), (4) and (5), the loss components are dependent either on torque T or speed ω as follows.

$$P_{Cu} = f(I^2) = f(T) \tag{6}$$

$$P_{Fe} = f\left(B_g, f_s\right) = f(\Phi_{PM}, f_s) = f(\omega) \tag{7}$$

$$P_{fw} = f(\omega) \tag{8}$$

In a particular laboratory test, the mechanical loss component P_{fw} is measured at variable rotor speed n in the full range of its change 0-4000 rpm; afterwards, the experimentally obtained curve is approximated with high accuracy by a polynomial of the 5^{th} order of $n \equiv \omega$, where:

$$\omega\ (\text{rad/s}) = \frac{2\pi}{60} \cdot n\ (\text{rpm}) \tag{9}$$

Consequently, the equation for calculation of the total loss, in dependence of torque T and speed ω, is done by:

$$P_{loss} = P_{Cu} + P_{Fe} + P_{fw} = f(T, \omega) \tag{10}$$

Finally, the eq. (1) becomes:

$$\eta(T, \omega) = \frac{T \cdot \omega}{T \cdot \omega + P_{loss}(T, \omega)} \tag{11}$$

Thanks to the availability of measured data for the motor, the outcomes are verified with reliable indicators, enabling to prove the proposed methodology and two motor models as accurate. Thus the LF model makes it possible a very fast calculation of the motor parameters due to the procedure relying on simplified mathematical operations, while the HF model, which is based on a reduced number of FE analyses, ensures a validation of the obtained results.

FEM results for the studied motor are obtained in a 2D domain by means of a 2D magnetostatic techniques [5]. In Fig. 3 a detail of the mesh (a) and the no-load magnetic field distribution (b) of PMSM, at the initial rotor position 0°, when the axis of resultant stator field and permanent magnet north pole axis are aligned, are shown.

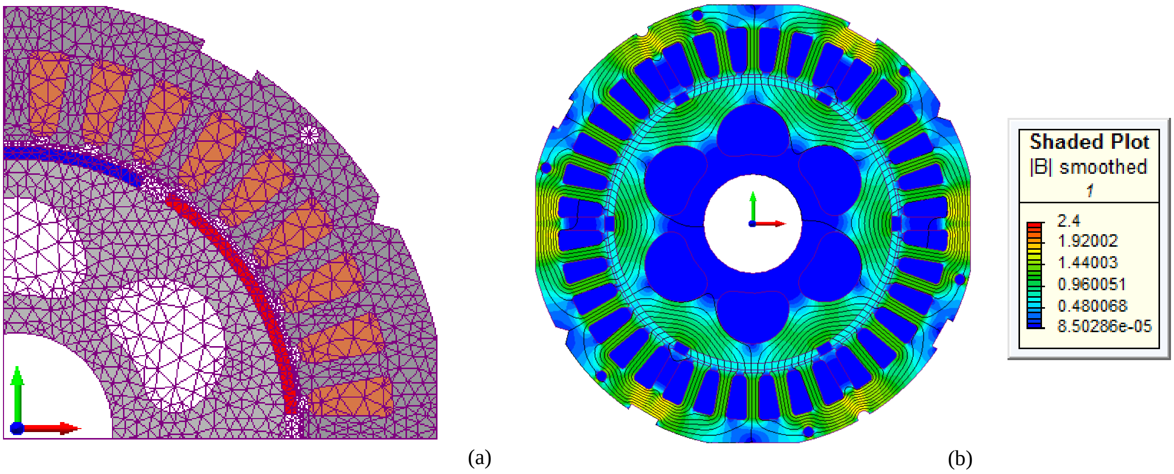

Fig. 3. Detail of the FEM mesh (a) and magnetic field distribution at no-load and initial position of PMSM (b).

To complete the numerical experiment of the studied motor, the calculations at rated load operation have been performed. The three stator phase windings are supplied by rated current with rectangular waves, as follows [6]: $I_A = +I_n$, $I_B = -I_n$, while $I_C = 0$. The magnetic field distribution for the rotor position where both the permanent magnet north pole axis and the armature field north pole axis are aligned with d-axis of the motor topology is presented in Fig. 4 (a); in Fig. 4 (b) is given the magnetic field distribution when the rotor is displaced along q-axis of the motor, which is equivalent to an angle of 30° mech. i.e. 90° electrical. In this case, both the field axes are in quadrature.

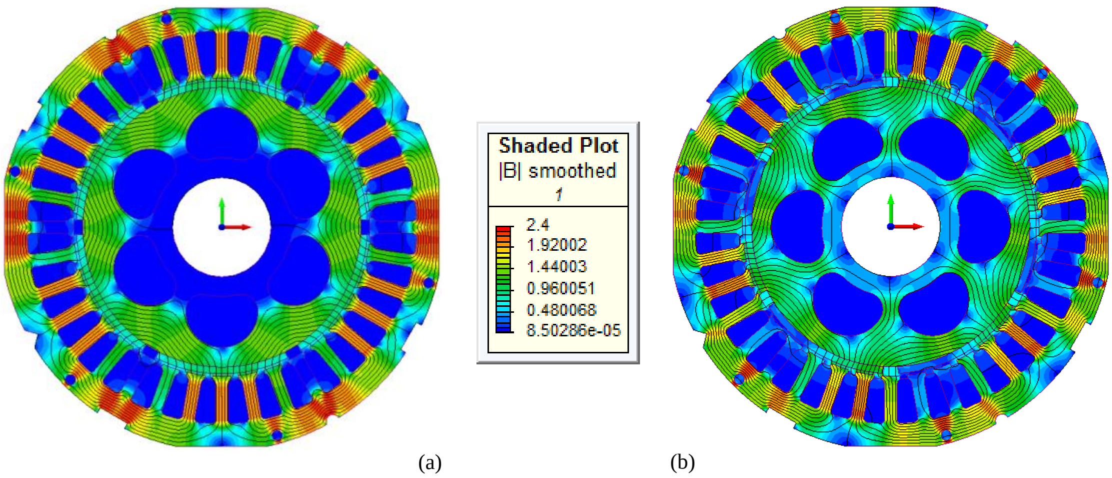

Fig. 4. Magnetic field distribution at rated load: initial rotor position 0^0 (a) and 90^0 electrical (b).

In Table I several of the analytically computed quantities are comparatively presented, along with measured and, where applicable, FEA ones. Based on Table I, the results obtained by the analytical motor model evidently show a very good agreement.

Table I - Comparison of Results

Quantity \ Method	Analytical	Measured	FEA
Phase current (A)	17.705	17.6	input value
Line-to-line voltage (V)	45.5	42.0	44.57
Air-gap flux linkage (Vs)	0.1332	0.1261	0.1251
Iron loss (W)	17.36	-	19.13
Copper loss	147.09	140.81	-
Total loss	186.45	188.0	-
Efficiency at rated load	0.849	0.848	-

Efficiency map calculation

As proved before, the LF model of the PMSM gives fast results at satisfactory accuracy. A sequence of calculations of the motor efficiency are accomplished. In particular, two families of charts η=f(T) at n=const. and η=f(n) at T=const., have been created; they are presented in Fig. 5 (a) and 5 (b), respectively. The charts show the bounds of the efficiency change, for any arbitrary selected value for torque T and speed n.

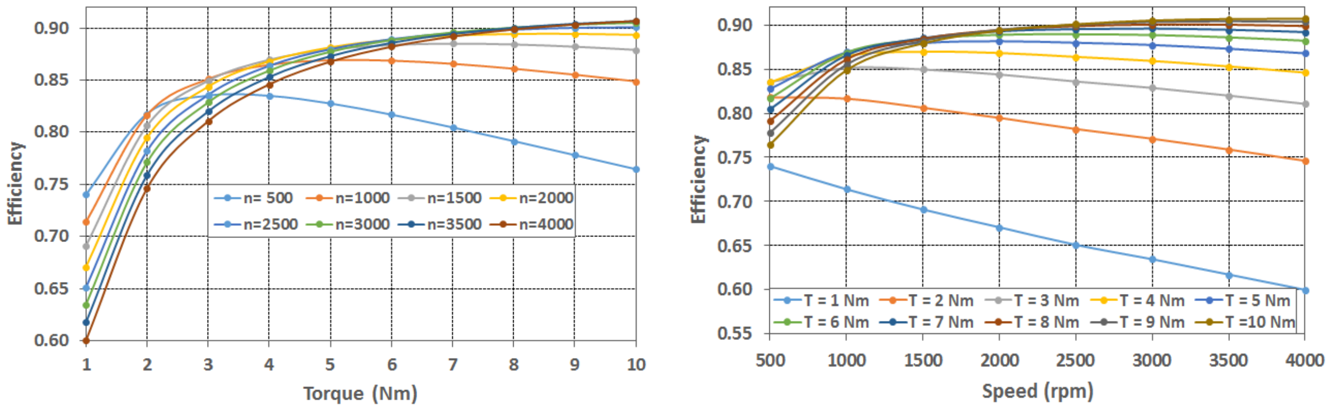

(a) (b)

Fig. 5. Charts η = f(T) at n=const (a), η = f(n) at T=const (b).

From this point on, the curves from low-fidelity (LF) motor model, as seen in Fig. 5 (a) and (b), are utilised in order to set up the efficiency map synthesis and the optimisation problem solution. One possible approach is to combine the charts (a and (b) and to derive the efficiency map η = f(T,n) in the whole T×n space. The drawback of this procedure is the lack of accuracy and reliability. This way, given a feasible geometry of PMSM, the LF model makes it possible to quickly synthesise the relevant efficiency map.

In [7], for instance, a high-fidelity (HF) neural metamodel for computing the efficiency map is presented, but the bottleneck is the highest number of FEA needed to form the training data set. The time consumption is a major drawback of this approach.

As a good compromise, in this research, a variable-fidelity (VF) model is proposed. It is a unique combination of the analytical model and numerical motor models. Thus, for preselected efficiency value, the VF model makes possible relatively fast and accurate simulation of a family of torque-speed curves of the studied PMSM.

Optimization problem

In order to improve the motor performance in terms of efficiency, it is important to enlarge the region in the torque-speed plane in which the efficiency is higher than the rated value; in fact, this situation ensures quite a wide range of working points. In contrast, maximising only the rated value of the efficiency could lead to a very good performance, but characterized by a working point in a narrow operating area the torque-speed space.

Following this remark, the optimization problem reads as follows: *starting from an initial geometry of PMSM, find the geometry such that the area encompassed by the contour line corresponding to the rated value of efficiency η_n is maximum, subject to the problem constraints*. In particular, the optimisation target is to maximise the feasible area of the efficiency η with $\eta \geq \eta_n$, being η_n=0.85 the rated value of the efficiency.

The design variables ruling the motor geometry are: the rotor radius R_R, the air gap length g, the permanent magnet height (length) l_m, the permanent magnet pole coverage f_m and the axial length of the motor L, as sketched in Fig. 6.

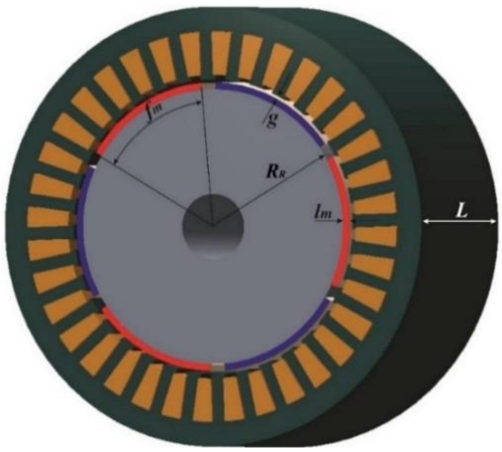

Fig. 6. Sketch of the design variables

The variation range for each design variable is show in Table II.

Table II - Variation range for the design variables

Design variable	Lower value	Higher value
R_R (mm)	35.7	48.3
g (mm)	0.68	0.92
l_m (mm)	1.70	2.30
f_m (/)	0.77	1
L (mm)	76.5	103.5

In order to maximise the objective function, a lowest-order algorithm of evolutionary computing governs the search, in particular, the *EStra* method, which has been proven to be well effective and highly reliable is used [8,9].

It is interesting to note that the computational burden is substantial, in fact, for each set of design variables and so for each geometry originated by the optimization algorithm, the relevant efficiency map should be recomputed. Hence, the use of the LF model is preferable in view of a fast optimization process.

Optimization results

For solving the optimization problem, the EStra method is applied, starting from the prototype in Table II, in the limit of 80 iterations; for each geometry dictated by the algorithm, the relevant analysis problem is solved by means of the low fidelity model. The optimization results are shown in Table III.

Table III - Starting point and optimal solution of the optimization procedure

Design variable	Initial solution	Optimal solution
R_R (mm)	42.2	40.5
g (mm)	0.80	0.70
l_m (mm)	2.0	2.2
f_m (/)	0.9	0.825
L (mm)	90.0	103.2
Objective function: Area η ≥ 0.85	**14.6×10^3**	**26.5×10^3**

In Fig. 7 (a) and 7 (b) the efficiency maps for the initial solution and the optimal solution of the PMSM are shown, respectively.

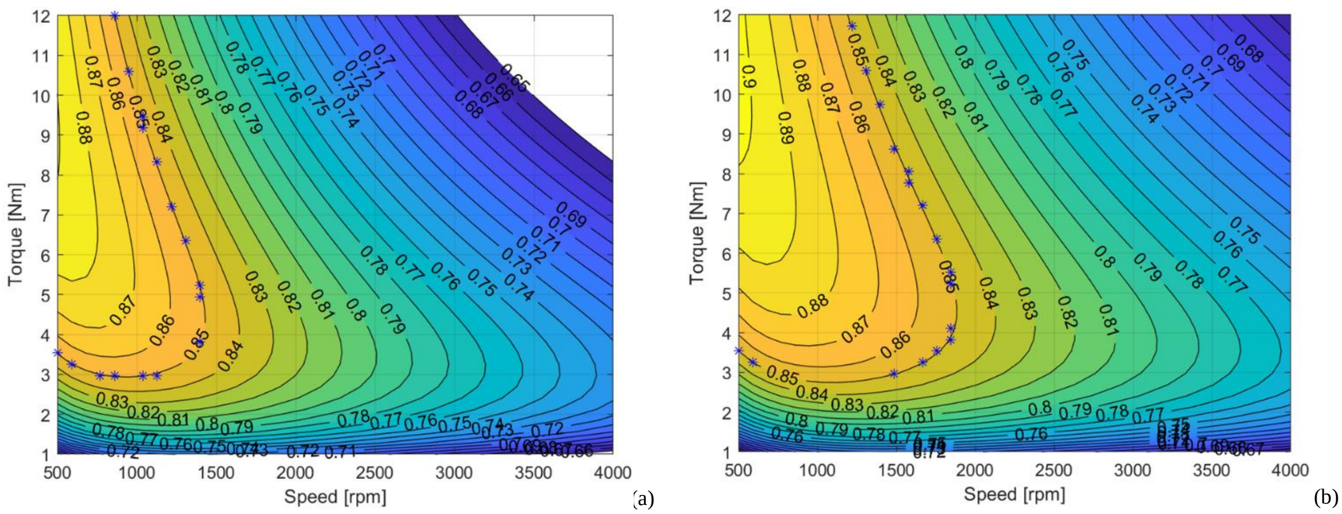

Fig. 7. Efficiency map of the initial solution (a), and optimal solution (b).

In Fig. 7 the blue asterisks highlight the area for which $\eta \geq \eta_n$ i.e. $\eta \geq 0.85$. As can be noted from Fig. 7 (b), this area for the optimized solution is substantially wider than the one of the initial solution, as seen in Fig. 7 (a). Therefore, the optimisation target has been achieved: in fact, the feasible area where efficiency is higher than the rated value, is increased from 14.6×10^3 to 26.5×10^3; correspondingly, as seen in the Table III, the objective function is increased for more than 1.8 times.

A further remark can be put forward: knowing that the copper loss is the dominant component of the total motor loss and in turn with major influence on the efficiency value, the current density maps are computed for both initial and optimal solutions (see Fig. 8). It is obvious that allowed operating region, for $J \leq J_{max} = 7$ A/mm^2 (white area on the charts), is extended towards higher speed and bigger torque values. At the same time, the forbidden region where $J \geq 7$ (A/mm^2) is significantly decreased. This is an excellent side-benefit of the area formulation here adopted, because current densities exceeding the maximum allowed value for the respective insulation class of the motor would produce overheating and temperature rise that will certainly damage the motor.

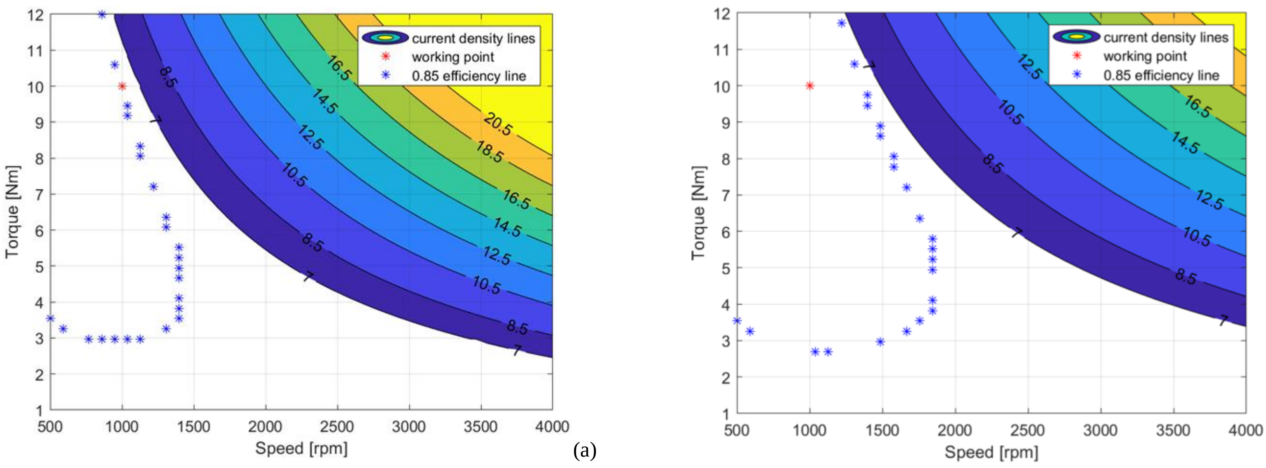

Fig. 8. Contour of the efficiency map (η =0.85, blue asterisks) of the initial solution (a), and optimal solution (b): the current density is mapped with coloured areas, the working point is represented with a red asterisk.

From Fig. 8, it can be also noted that the η=0.85 efficiency line expands, during the optimization procedure, in a way the working point is located inside the interior region. Correspondingly, the region of high current density is shifted far from the working point (see initial point, Fig. 8a versus optimal solution, Fig. 8b). This is clearly an advantage because the working point for the optimized solution is set in a region of the torque-speed plane where the copper losses are lower than those of the initial motor for the same working point.

Following a similar criterion of *a posteriori* analysis, in Fig. 9 the copper loss chart is plotted in the torque-speed space and for a sake of a comparison the contour of the efficiency map at η=0.85 is drawn as well.

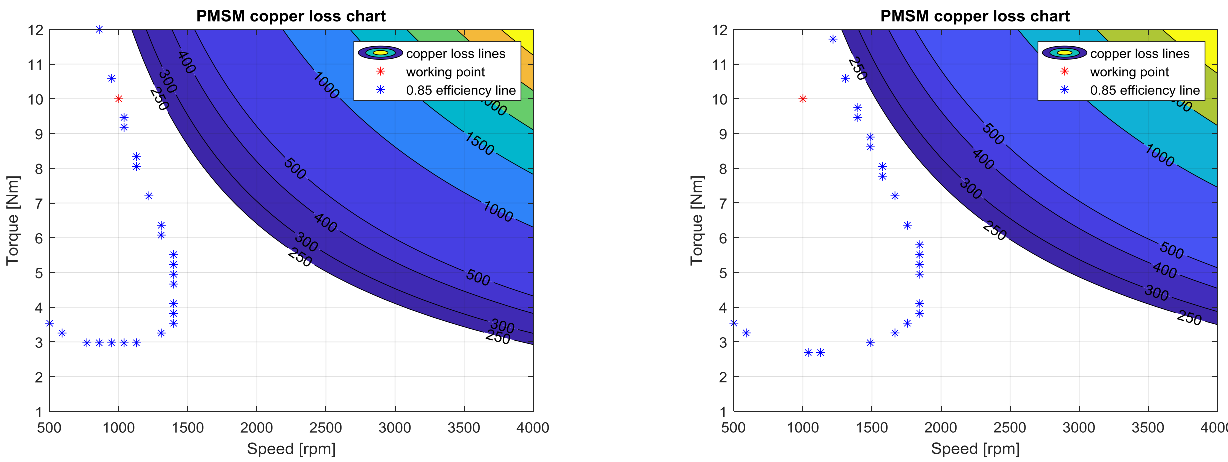

(a) (b)

Fig. 9. Contour of the efficiency map (η =0.85, blue asterisks) of the initial solution (a), and optimal solution (b): the copper loss is mapped with coloured areas, the working point is represented with a red asterisk.

It can be noted that the working point which corresponds to the prototype solution (Fig. 9a) is located close to the region of high loss, while the high-loss region is shifted far from the working point as a result of the design optimization (Fig. 9b).

Conclusion

An original approach to efficiency map synthesis of a permanent magnet motor, where the goal is an extension of a specific map area for a given value of the efficiency, is presented. A controlled permanent motor is selected as the case study. The range of torque control 0-10 Nm, as well as 0-4000 rpm range for speed control define the space where the optimisation of the efficiency map is done.

An analytical low-fidelity model of the motor has been developed; its accuracy was tested and proved by using the values obtained from the laboratory measurements and numerical FEA experiments. A variable-fidelity model, based on a circuit-field approach, makes possible a fast and accurate simulation of a family of torque-speed curves for the PMSM. Accordingly, the optimal synthesis of the relevant efficiency map has been achieved, where the end-target was to maximise the area encompassed by a predefined (usually rated) value for the motor efficiency. A sequence of candidate solutions determine the objective function space, while the set of variables – defining the best objective function value – determine the new PMSM motor geometry. The optimisation results, along with the values of the existing (initial) motor model, are presented in tables and charts.

Based on the performed analyses, the proposed modelling, as well as the original strategy for optimising and shaping efficiency map, has been proved to be efficient, accurate and reliable.

References

[1] P. Di Barba, M.E. Mognaschi, N. Rezaei, D.A. Lowther, T. Rahman, "Many-objective shape optimisation of IPM motors for electric vehicle traction", International Journal of Applied Electromagnetics and Mechanics, 60 (S1), 2019, pp. S149-S162.

[2] L. Petkovska and G. Cvetkovski, "Assessment of Torques for a Permanent Magnet Brushless DC Motor Using FEA, Przeglad Elektrotechniczny, Vol. 87, No. 12b, pp. 132-136, December 2011.

[3] D. Stoia, M. Cernat, A. A. Jimor, D. V. Nicolae, "Analytical Design and Analysis of Line-Start Permanent Magnet Synchronous Motors", *Proceedings of IEEE AFRICON*'2009, 2009, pp. 1-6, Nairobi, Kenya

[4] Y. L. Karnavas, I. D. Chasiotis, C. D. Korkas, S. K. Amoutzidis, "Modelling and multiobjective optimization analysis of a permanent magnet synchronous motor design", *International Journal of Numerical Modelling (JNM)*, Vol. 30, No. 6, 2017, pp. 1-14, wileyonlinelibrary.com/journal/jnm, https://doi.org/10.1002/jnm.2232.

[5] https://www.plm.automation.siemens.com/global/en/products/simcenter/magnet.html.

[6] L. Petkovska, G. Cvetkovski, "Performance Analysis of a Surface Permanent Magnet Motor", *Journal Przeglad Elektrotechniczny*, Sigma Not, Vol. 92, NR. 12, 2016, pp. 133-136.

[7] A. Khan, M. H. Mohammadi, V. Ghorbanian and D. A. Lowther, "Efficiency Map Prediction of Motor Drives Using Deep Learning", IEEE Transactions on Magnetics, Vol. 56, No. 3, March 2020.

[8] P. Di Barba, M. E. Mognaschi, "Recent experiences of multiobjective optimisation in electromagnetics: A comparison of methods," *COMPEL*, Vol. 24, No. 3, 2005, pp. 921–930, doi: 10.1108/03321640510598238.

[9] P. Di Barba, M. E. Mognaschi, "Industrial Design With Multiple Criteria: Shape Optimization of a Permanent-Magnet Generator," *IEEE Transaction on Magnetics*, Vol. 45, No. 3, 2009, pp. 1482–1485, doi: 10.1109/TMAG.2009.2012685.